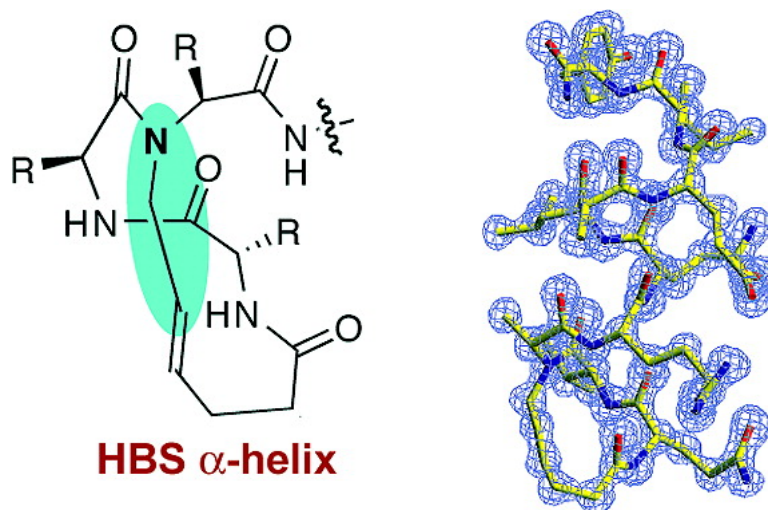


## Atomic Structure of a Short $\alpha$ -Helix Stabilized by a Main Chain Hydrogen-Bond Surrogate

Jie Liu, Deyun Wang, Qi Zheng, Min Lu, and Paramjit S. Arora

*J. Am. Chem. Soc.*, **2008**, 130 (13), 4334-4337 • DOI: 10.1021/ja077704u

Downloaded from <http://pubs.acs.org> on February 8, 2009



### More About This Article

Additional resources and features associated with this article are available within the HTML version:

- Supporting Information
- Links to the 1 articles that cite this article, as of the time of this article download
- Access to high resolution figures
- Links to articles and content related to this article
- Copyright permission to reproduce figures and/or text from this article

[View the Full Text HTML](#)

## Atomic Structure of a Short $\alpha$ -Helix Stabilized by a Main Chain Hydrogen-Bond Surrogate

Jie Liu,<sup>†</sup> Deyun Wang,<sup>‡</sup> Qi Zheng,<sup>†</sup> Min Lu,<sup>†</sup> and Paramjit S. Arora<sup>\*†</sup>

Department of Biochemistry, Weill Medical College of Cornell University, New York, New York 10021, and Department of Chemistry, New York University, New York, New York 10003

Received October 6, 2007; E-mail: arora@nyu.edu

**Abstract:** Herein we report the 1.15 Å X-ray crystal structure of a short  $\alpha$ -helix in which the N-terminal  $i$  and  $i + 4$  main chain hydrogen bond is replaced with a carbon–carbon bond. The structure shows that the hydrogen-bond surrogate (HBS) derived  $\alpha$ -helix truly resembles the structure of canonical  $\alpha$ -helices and provides unequivocal support for our helix nucleation strategy.

### Introduction

Stabilization of short peptides in  $\alpha$ -helical conformation remains a challenging endeavor. The helix–coil transition theory in peptides suggests that the energetically demanding organization of three consecutive amino acids into the helical orientation inherently limits the stability of short  $\alpha$ -helices.<sup>1–3</sup> According to this theory,  $\alpha$ -helices composed of 10 or less amino acids are expected to be essentially unstable due to a low nucleation probability.<sup>4,5</sup> We have described a method that affords preorganized  $\alpha$ -turns to overcome the nucleation barrier and initiate  $\alpha$ -helix formation.<sup>6–8</sup> We obtain preorganized  $\alpha$ -turns by replacing the N-terminal main chain hydrogen bond between the C=O of the  $i$ th amino acid residue and the NH of the  $i + 4$ th amino acid residue with a carbon–carbon bond (Figure 1a).<sup>9,10</sup>

A key feature of this hydrogen-bond surrogate (HBS) approach is that the internal placement of the cross-link affords short helices with minimal perturbations to their molecular recognition surfaces. Traditional helix stabilization methods have relied predominantly on side-chain constraints,<sup>11–14</sup> capping

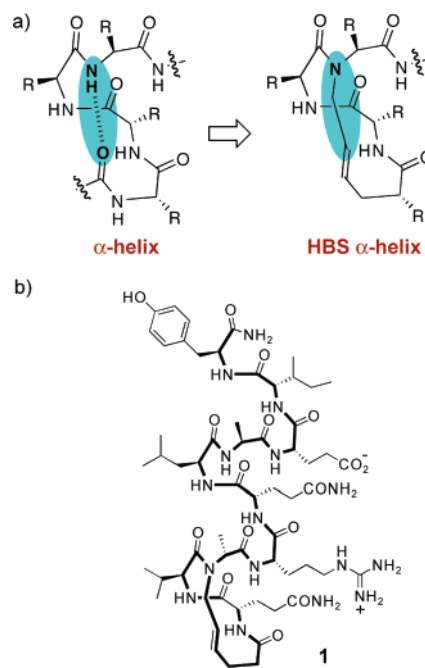


**Figure 1.** (a) Strategy for the stabilization of  $\alpha$ -helices by replacement of an  $i$  and  $i + 4$  hydrogen bond with a carbon–carbon bond to obtain a hydrogen-bond surrogate (HBS) based  $\alpha$ -helix. (b) Chemical structure of HBS  $\alpha$ -helix 1.

templates,<sup>15,16</sup> or nonnatural amino acid substitutions.<sup>17,18</sup> These methods either block solvent-exposed surfaces of the target  $\alpha$ -helices or remove important side-chain functionalities. The HBS strategy allows strict preservation of the helix surfaces. We have described an olefin metathesis-based strategy for the preparation of these artificial helices.<sup>9,10</sup> Our synthetic strategy utilizes standard Fmoc solid-phase peptide synthesis methodol-

<sup>†</sup> Weill Medical College of Cornell University.

<sup>‡</sup> New York University.

- (1) Lifson, S.; Roig, A. *J. Chem. Phys.* **1961**, *34*, 1963–1974.
- (2) Zimm, B. H.; Bragg, J. K. *J. Chem. Phys.* **1959**, *31*, 526–535.
- (3) Qian, H.; Schellman, J. A. *J. Phys. Chem.* **1992**, *96*, 3987–3994.
- (4) Siedlecka, M.; Goch, G.; Ejchart, A.; Sticht, H.; Bierzyński, A. *Proc. Natl. Acad. Sci. U.S.A.* **1999**, *96*, 903–908.
- (5) Yang, J. X.; Zhao, K.; Gong, Y. X.; Vologodskii, A.; Kallenbach, N. R. *J. Am. Chem. Soc.* **1998**, *120*, 10646–10652.
- (6) Chapman, R. N.; Dimartino, G.; Arora, P. S. *J. Am. Chem. Soc.* **2004**, *126*, 12252–12253.
- (7) Wang, D.; Chen, K.; Kulp, J. L., III; Arora, P. S. *J. Am. Chem. Soc.* **2006**, *128*, 9248–9256.
- (8) Wang, D.; Chen, K.; Dimartino, G.; Arora, P. S. *Org. Biomol. Chem.* **2006**, *4*, 4074–4081.
- (9) Chapman, R. N.; Arora, P. S. *Org. Lett.* **2006**, *8*, 5825–5828.
- (10) Dimartino, G.; Wang, D.; Chapman, R. N.; Arora, P. S. *Org. Lett.* **2005**, *7*, 2389–2392.
- (11) Blackwell, H. E.; Grubbs, R. H. *Angew. Chem., Int. Ed.* **1998**, *37*, 3281–3284.
- (12) Osapay, G.; Taylor, J. W. *J. Am. Chem. Soc.* **1992**, *114*, 6966–6973.
- (13) Phelan, J. C.; Skelton, N. J.; Braisted, A. C.; McDowell, R. S. *J. Am. Chem. Soc.* **1997**, *119*, 455–460.
- (14) Schafmeister, C. E.; Po, J.; Verdine, G. L. *J. Am. Chem. Soc.* **2000**, *122*, 5891–5892.

(15) Chakrabarty, A.; Doig, A. J.; Baldwin, R. L. *Proc. Natl. Acad. Sci. U.S.A.* **1993**, *90*, 11332–11336.

(16) Lyu, P. C.; Wemmer, D. E.; Zhou, H. X.; Pinker, R. J.; Kallenbach, N. R. *Biochemistry* **1993**, *32*, 421–425.

(17) Kaul, R.; Balaran, P. *Bioorg. Med. Chem.* **1999**, *7*, 105–117.

(18) Lyu, P. C.; Sherman, J. C.; Chen, A.; Kallenbach, N. R. *Proc. Natl. Acad. Sci. U.S.A.* **1991**, *88*, 5317–5320.

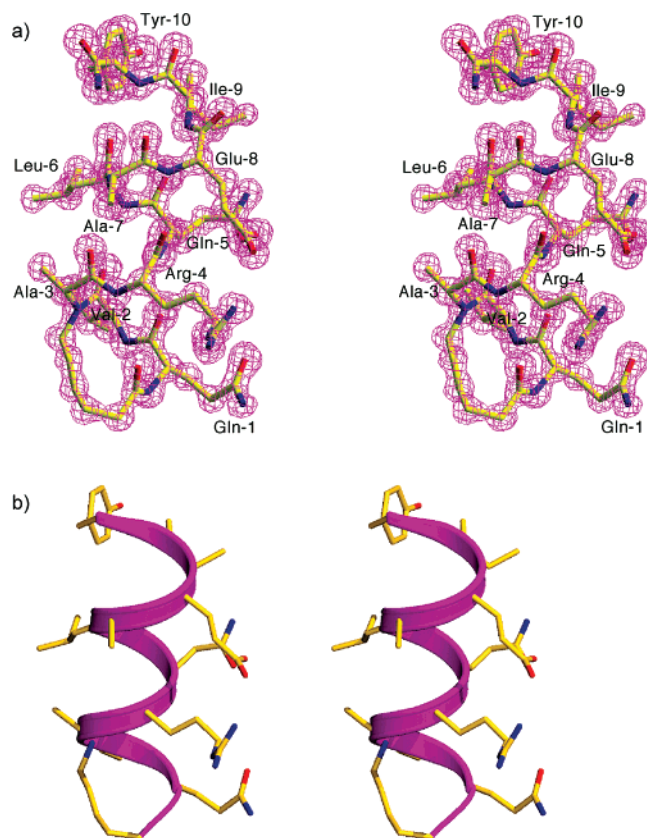


**Figure 2.** Crystal structure of the HBS  $\alpha$ -helix **1**. (a) Stereoview of the 1.15 Å  $2F_o - F_c$  electron density map (contoured at 1.5s) superimposed onto the refined molecular model. (b) Ribbon diagram of HBS helix **1**. The C $\alpha$  backbone of the  $\alpha$ -helix is depicted as a pink ribbon. Side chains of residues are shown. All carbon, nitrogen, and oxygen atoms are shown in yellow, blue, and red, respectively. Figures were created with the programs SETOR (ref 26), MOLSCRIPT (ref 27), and Raster 3D (ref 28).

ogy, resins, and reagents, and provides HBS helices in sufficient amounts for subsequent biophysical and biological analyses. Importantly, we have shown that HBS  $\alpha$ -helices can bind their expected protein receptors with high affinities and can inhibit complex protein–protein interactions in cell culture.<sup>19,20</sup>

In previous reports, we demonstrated that the HBS  $\alpha$ -turn can stabilize  $\alpha$ -helical structure in short alanine-rich<sup>6</sup> and biologically relevant sequences.<sup>7</sup> In this report we present the X-ray crystal structure of an HBS  $\alpha$ -helix at 1.15 Å resolution. The structure of the helix superimposes well onto a model of an idealized  $\alpha$ -helix, supporting our hypothesis that stable short helices can be accessed by the HBS strategy. As crystal structures of short  $\alpha$ -helices have been typically reported with the  $\alpha$ -helix in complex with a protein partner,<sup>21–25</sup> we believe that the solid-state structure of an isolated short helix suggests a high degree of conformational stability being conferred by

**Table 1.** Crystallographic Data and Refinement Statistics for Helix **1**

(A) Data Collection Statistics	
temperature (K)	100
X-ray source	NSLS X4A
space group	$P2_1$
cell dimensions	$a = 16.35 \text{ \AA}$ , $b = 10.71 \text{ \AA}$ , $c = 44.10 \text{ \AA}$ , $\beta = 98.5^\circ$
molecules in the asymmetric unit	2
solvent content (%)	20
resolution (Å)	43.6–1.15
no. of total reflections	26 226
no. of unique reflections	4737
multiplicity	5.5
data completeness (%)	82.5 (98.0) <sup>a</sup>
$I/\sigma_I$	12.2
$R_{\text{merge}} (\%)^b$	5.7
(B) Refinement Statistics	
non-hydrogen atoms	
protein	182
water	15
resolution (Å)	43.6–1.15
$R_{\text{cryst}}/R_{\text{free}} (\%)^c$	14.9/17.0
rms deviations from ideality	
bond lengths (Å)	0.027
bond angles (deg)	2.7
torsion angles (deg)	6.8
average $B$ -factors (Å <sup>2</sup> )	7.7
protein	7.2
water	13.8
estimated error for $B$ -factors (Å <sup>2</sup> )	0.5

<sup>a</sup> Value in parentheses refers to data completeness in the resolution range 43.6–1.15 Å. <sup>b</sup>  $R_{\text{merge}} = \sum_{hkl} \sum_i |I_i - \langle I \rangle| / \sum_{hkl} \sum_i I_i$ , where  $I_i$  is the intensity for the  $i$ th measurement of an equivalent reflection with indices  $h, k, l$ . <sup>c</sup>  $R_{\text{cryst}} = \sum |F_{\text{obs}} - F_{\text{calc}}| / \sum F_{\text{obs}}$ ,  $R_{\text{free}} = R_{\text{cryst}}$  calculated using 10% of the reflection data chosen randomly and omitted from the start of refinement.

the HBS strategy. Thermal and chemical denaturation studies also show that pre-nucleated HBS  $\alpha$ -helices are exceptionally stable.<sup>6–8</sup>

## Results and Discussion

The chemical structure and the high-resolution crystal structure of HBS  $\alpha$ -helix **1** are shown in Figures 1b and 2, respectively. The sequence of this helix is derived from the proapoptotic protein Bak BH3, and its solution conformation was previously characterized by NMR spectroscopy.<sup>7,8</sup> We have also demonstrated that a longer analog of this HBS  $\alpha$ -helix can target its expected protein receptor, Bcl-xL, with high affinity.<sup>19</sup> The only difference between the compound that crystallized and the one studied by NMR is the stereochemistry of alanine-3 in the peptide sequence (Q<sub>1</sub>V<sub>2</sub>A<sub>3</sub>R<sub>4</sub>Q<sub>5</sub>L<sub>6</sub>A<sub>7</sub>E<sub>8</sub>I<sub>9</sub>Y<sub>10</sub>-NH<sub>2</sub>). Our synthetic methodology results in some epimerization at the alanine-3 position. We can separate the resulting diastereomers by HPLC and establish stereochemistry by NMR (see the Supporting Information for details). A pure sample consisting of natural amino acids was used for the NMR studies. The HBS helix **1** containing D-alanine-3 provided the best crystal and is described here. The stereochemical switch at the 3-position does not cause any apparent distortion in the HBS helix.

Compound **1** was crystallized at room temperature using the hanging drop vapor diffusion method by equilibrating against reservoir buffer (100 mM sodium citrate (pH 5.6), 20% PEG 4000, 18% isopropyl alcohol) a solution containing 1  $\mu$ L of 15 mg mL<sup>-1</sup> peptide in 20% acetic acid and 1  $\mu$ L of reservoir buffer. The crystals belong to the space group  $P2_1$  with unit cell dimensions of  $a = 16.35 \text{ \AA}$ ,  $b = 10.71 \text{ \AA}$ ,  $c = 44.10 \text{ \AA}$ ,  $\beta$

(19) Wang, D.; Liao, W.; Arora, P. S. *Angew. Chem., Int. Ed.* **2005**, *44*, 6525–6529.

(20) Wang, D.; Lu, M.; Arora, P. S. *Angew. Chem., Int. Ed.* **2008**, *47*, 1879–1882.

(21) Kim, E. E.; Varadarajan, R.; Wyckoff, H. W.; Richards, F. M. *Biochemistry* **1992**, *31*, 12304–12314.

(22) Kussie, P. H.; Gorina, S.; Marechal, V.; Elenbaas, B.; Moreau, J.; Levine, A. J.; Pavletich, N. P. *Science* **1996**, *274*, 948–953.

(23) Sia, S. K.; Carr, P. A.; Cochran, A. G.; Malashkevich, V. N.; Kim, P. S. *Proc. Natl. Acad. Sci. U.S.A.* **2002**, *99*, 14664–14669.

(24) Karle, I. L.; Flippenanderson, J. L.; Uma, K.; Balaram, H.; Balaram, P. *Proc. Natl. Acad. Sci. U.S.A.* **1989**, *86*, 765–769.

(25) Yang, D. S. C.; Sax, M.; Chakrabarty, A.; Hew, C. L. *Nature* **1988**, *333*, 232–237.

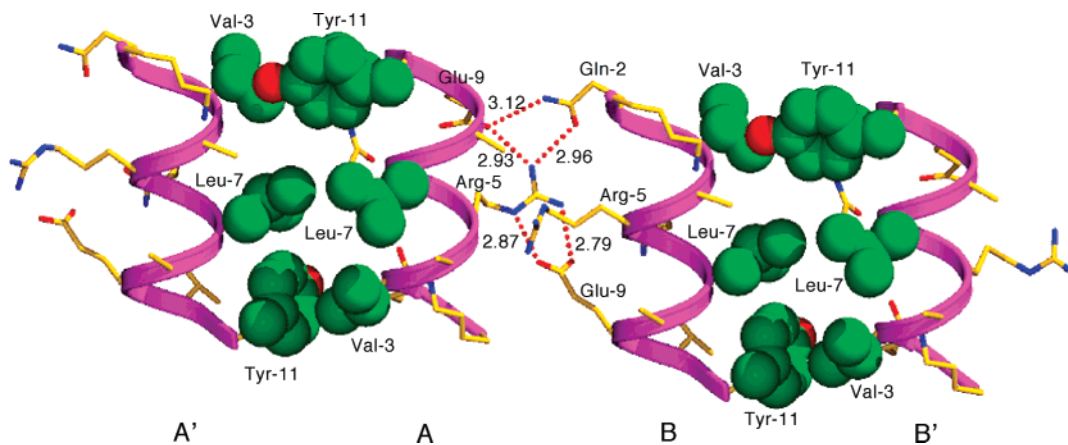


**Figure 3.** Crystal packing in the HBS helix **1** structure. Potential hydrogen bonds between helices A and B in the unit cell are shown as dashed lines. Hydrogen-bond distances are given in angstroms. Residues forming van der Waals interactions between the symmetry-related A/A' and B/B' helices are indicated.

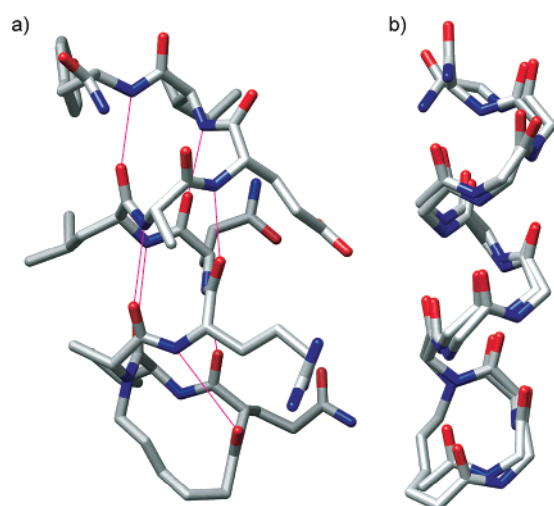


**Figure 4.** (a) Putative  $i$  and  $i + 4$  hydrogen bonds (magenta lines) in the crystal structure-derived molecular model of **1**. (b) Overlay of the crystal structure and a model of an idealized  $\alpha$ -helix.

$= 98.5^\circ$ . Crystallographic data and refinement statistics are shown in Table 1.

Crystals of HBS  $\alpha$ -helix **1** contained two monomers in an asymmetric unit (Figure 3). The monomers interact through ionic and hydrogen-bonding interactions between arginine, glutamine, and glutamic residues from adjacent molecules and by potential van der Waals interactions between valine, leucine, and tyrosine residues in symmetry-related helices. The stabilizing hydrophobic interaction between the symmetry-related helices involves  $i$ ,  $i + 4$ , and  $i + 8$  residues, which is distinct from the hydrophobic interactions in classical coiled-coil motifs based on a heptad repeat ( $i$ ,  $i + 4$ , and  $i + 7$  residues) at the interface.

All  $i$  and  $i + 4$  C=O and NH hydrogen-bonding partners fall within distances and angles expected for a fully hydrogen-bonded short  $\alpha$ -helix (Figure 4a). The backbone conformation of **1** in the crystal structure superimposes with an rms difference of 0.75 Å onto the backbone conformation of a model  $\alpha$ -helix of sequence AcQVARQLAEIY-NH<sub>2</sub> (Figure 4b). Backbone torsion angles for **1** are listed in Table 2. The average  $\phi$  ( $-55^\circ$ ) and  $\psi$  ( $-40^\circ$ ) values for residues within the helix fall within the range expected for a canonical  $\alpha$ -helix. Table 2 also describes the crystal structure derived rise per residue along the helix axis together with extrapolated number of residues per

**Table 2.** Structural Parameters of HBS  $\alpha$ -helix **1**

residue	$\phi$ (deg)	$\psi$ (deg)	$\omega$ (deg)	rise per residue, $h$ (Å) <sup>a</sup>	residues per $\alpha$ -helical turn, $n^b$
ideal $\alpha$ -helix	$-57$	$-47$	$180$	$1.50$	$3.60$
Gln-1	$113$	$-46$	$-169$		
Val-2	$-71$	$-47$	$176$	$1.45$	$3.82$
Ala-3	$-55$	$-45$	$-177$	$1.50$	$3.64$
Arg-4	$-58$	$-40$	$-178$	$1.58$	$3.61$
Gln-5	$-69$	$-40$	$176$	$1.54$	$3.65$
Leu-6	$-63$	$-37$	$180$	$1.48$	$3.64$
Ala-7	$-67$	$-39$	$-176$	$1.48$	$3.72$
Glu-8	$-77$	$-27$	$-178$	$1.34$	$4.00$
Ile-9	$-91$	$-55$	$-165$	$1.21$	$4.27$
Tyr-10	$-110$	$-24$			

<sup>a</sup> Rise along the helix axis from the previous residue. <sup>b</sup>  $\alpha$ -Helical parameters were calculated using TWISTER (ref 29).

$\alpha$ -helical turn. These values provide important insight into the structure adopted by these engineered helices, suggesting that the helix begins to slightly unwind one helical turn away from the macrocycle. Conversely, the unfolding of the helix, as monitored by circular dichroism spectroscopy, remains highly cooperative up to a temperature of 95 °C in aqueous solutions.<sup>7,8</sup>

We had previously derived a solution structure of HBS  $\alpha$ -helices from circular dichroism and NMR spectroscopies.<sup>7</sup> (An overlay of the HBS helix structures derived from X-ray crystallography and NMR spectroscopy is included in the Supporting Information, Figure S3.) Although these methods provide useful information concerning the conformation adopted by HBS helices, the crystal structure provides atomic level details of the conformation unique to X-ray crystallography. For example, direct measurements of the  $\psi$  angles and helix rise per residue values are not possible from NMR spectroscopy. Significantly, we were unable to fully define the conformation adopted by the HBS macrocycle by NMR spectroscopy due to the severe spectral overlap of the protons in the hydrocarbon bridge and in the side chains of aliphatic amino acids. We developed a semiquantitative model for the nucleation macrocycle from the limited set of nonoverlapping NOEs, which suggested that the macrocycle might be strained and the design may need to be further refined.<sup>8</sup> The crystal structure clearly shows that the HBS macrocycle is well-defined with the carbonyls of the macrocycle participating in all potential  $i$  and

$i + 4$  hydrogen bonds. The crystal structure uniquely shows both the nucleation site and the details of the helix conformation at 1.15 Å resolution.

It is interesting to note that the HBS helix tolerates a D-amino acid in the middle of the sequence because typically D-amino acids are considered to destabilize  $\alpha$ -helix or favor the left-handed conformation.<sup>30–32</sup> The Ramachandran space for an L-amino acid in a right-handed  $\alpha$ -helix is small, but it is sterically allowed; the reverse should hold for D-amino acids.<sup>33,34</sup> Recent work by Sakurai et al. suggests that a peptide composed of D-amino acids may in fact adopt a two-turn right-handed  $\alpha$ -helical conformation.<sup>35</sup> Studies to examine the tolerance for D-amino acids at other positions in HBS helices and the proteolytic stability of the resulting chimeric constructs are underway.

## Conclusions

The 1.15 Å X-ray crystal structure provides unequivocal support for our hypothesis that replacement of the hydrogen bond between the  $i$  and  $i + 4$  residues at the N-terminus of a short peptide with a carbon–carbon bond results in a highly stable constrained  $\alpha$ -helix. Importantly, the crystal structure shows that the alkene-based macrocycle faithfully reproduces the conformation of a pre-nucleated  $\alpha$ -turn. Given the paucity of the X-ray structures of short  $\alpha$ -helices in the literature, and the importance of this motif in biology, we believe that this result will be of interest to the wider bioorganic chemistry community.

## Experimental Section

**Structure Determination.** The HBS  $\alpha$ -helix was crystallized at room temperature using the hanging drop vapor diffusion method by equilibrating against reservoir buffer (100 mM sodium citrate (pH 5.6),

20% PEG 4000, 18% isopropyl alcohol) a solution containing 1  $\mu$ L of 15 mg mL<sup>-1</sup> peptide in 20% acetic acid and 1 mL of reservoir buffer. The crystals were transferred into cryosolution containing 100 mM sodium citrate (pH 5.6), 15% PEG 4000, 15% isopropyl alcohol, 20% glycerol, harvested, and frozen in liquid nitrogen. Diffraction data were collected on beamline X4A at the National Synchrotron Light Source. Reflection intensities were integrated and scaled with DENZO and SCALEPACK.<sup>36</sup> Initial phases were determined by molecular replacement with Phaser<sup>37</sup> using an idealized  $\alpha$ -helix model in a combined rotation–translation search. Two  $\alpha$ -helix model molecules were oriented and placed in the asymmetric unit, corresponding to the two  $\alpha$ -helix chains. This model and the data set for the HBS  $\alpha$ -helix were directly fed to Arp/Warp,<sup>38</sup> which provided a largely complete asymmetric unit of the two chains and allowed ~90% of the final model to be interpreted. The resulting experimental electron density map was of excellent quality and showed the location of all of the side chains. Crystallographic refinement of the HBS  $\alpha$ -helix structure was carried out using Refmac.<sup>39</sup> Density interpretation and manual model building were done with O.<sup>40</sup> All residues but two (IleA10 and IleB10) occupy the most preferred regions of the Ramachandran plot. IleA10 and IleB10 lie in allowed regions of the Ramachandran space.

CCDC 675526 contains atomic coordinates for HBS  $\alpha$ -helix **1**. These data can be obtained free of charge from The Cambridge Crystallographic Data Centre via [www.ccdc.cam.ac.uk/data\\_request/cif](http://www.ccdc.cam.ac.uk/data_request/cif).

**Acknowledgment.** P.S.A. is grateful for financial support from the NIH (GM073943), Research Corporation (Cottrell Scholar Award), and NYU (Whitehead Fellowship). We thank the NSF for equipment Grants MRI-0116222 and CHE-0234863, and the NCR/NIH for Research Facilities Improvement Grant C06 RR-16572. M.L. thanks the NIH (AI42382) and the Irma T. Hirsch Trust for financial support.

**Supporting Information Available:** Synthesis and characterization of HBS  $\alpha$ -helix **1**. This material is available free of charge via the Internet at <http://pubs.acs.org>.

JA077704U

(26) Evans, S. V. *J. Mol. Graphics* **1993**, *11*, 134 ff.

(27) Kraulis, P. J. *J. Appl. Crystallogr.* **1991**, *24*, 946–950.

(28) Merritt, E. A.; Murphy, M. E. P. *Acta Crystallogr., Sect. D* **1994**, *50*, 869–873.

(29) Strelkov, S. V.; Burkhard, P. J. *Struct. Biol.* **2002**, *137*, 54–64.

(30) Chen, Y.; Mant, C. T.; Hodges, R. S. *J. Peptide Res.* **2002**, *59*, 18–33.

(31) Fairman, R.; Anthonycahill, S. J.; Degrado, W. F. *J. Am. Chem. Soc.* **1992**, *114*, 5458–5459.

(32) Bang, D.; Gribenko, A. V.; Tereshko, V.; Kossiakoff, A. A.; Kent, S. B.; Makhatadze, G. I. *Nat. Chem. Biol.* **2006**, *2*, 139–143.

(33) Ramachandran, G. N.; Sasisekharan, V. *Adv. Protein Chem.* **1968**, *23*, 283–438.

(34) Aravinda, S.; Shamala, N.; Desiraju, S.; Balaram, P. *Chem. Commun.* **2002**, 2454–2455.

(35) Sakurai, K.; Chung, H. S.; Kahne, D. *J. Am. Chem. Soc.* **2004**, *126*, 16288–16289.

(36) Otwinowski, Z.; Minor, W. *Methods Enzymol.* **1997**, *276*, 307–326.

(37) Storoni, L. C.; McCoy, A. J.; Read, R. J. *Acta Crystallogr., Sect. D* **2004**, *60*, 432–438.

(38) Lamzin, V. S.; Wilson, K. S. *Acta Crystallogr., Sect. D* **1993**, *49*, 129–147.

(39) Murshudov, G. N.; Vagin, A. A.; Dodson, E. J. *Acta Crystallogr., Sect. D* **1997**, *53*, 240–255.

(40) Jones, T. A.; Zou, J. Y.; Cowan, S. W.; Kjeldgaard, M. *Acta Crystallogr., Sect. A* **1991**, *47*, 110–119.